JACS
JOURNAL OF THE AMERICAN CHEMICAL SOCIETY

Communication

pubs.acs.org/JACS

Highly Sensitive Coherent Anti-Stokes Raman Scattering Imaging of Protein Crystals

Grigory M. Arzumanyan,*[,†,‡] Nelya V. Doroshkevich,[†] Kahramon Z. Mamatkulov,[†] Sergey N. Shashkov,[§] Egor V. Zinovev,[⊥] Alexey V. Vlasov,[⊥] Ekaterina S. Round,[⊥,∥,∇] and Valentin I. Gordeliy*[,⊥,∥,∇]

[†]Joint Institute for Nuclear Research, 141980 Dubna, Russia

[‡]Dubna State University, 19 Universitetskaya st., Dubna 141982, Russia

[§]SOL Instruments, 220005 BY P.O. Box 235, Minsk, Republic of Belarus

[⊥]Moscow Institute of Physics and Technology, 141700 Dolgoprudny, Moscow region, Russia

[∥]Institut de Biologie Structurale J.-P. Ebel, Université Grenoble Alpes-CEA-CNRS, F-38000 Grenoble, France

[∇]Institute of Complex Systems: Structural Biochemistry (ICS-6), Research Centre Jülich, 52425 Jülich, Germany

Supporting Information

ABSTRACT: Serial crystallography at last generation X-ray synchrotron sources and free electron lasers enabled data collection with micrometer and even submicrometer size crystals, which have resulted in amazing progress in structural biology. However, imaging of small crystals, which although is highly demanded, remains a challenge, especially in the case of membrane protein crystals. Here we describe a new extremely sensitive method of the imaging of protein crystals that is based on coherent anti-Stokes Raman scattering.

Water soluble and membrane proteins (MPs) are the functional units within cells. MPs serve vital functions such as ion and solute transport, energy and sensory transduction and represent roughly one-third of the proteins encoded in the human genome.[1] However, although they are also extremely important drug targets (up to 60% of all existing drugs target MPs) they remain poorly characterized both functionally and structurally.[2] Their crystallization and therefore structural investigation is still a great challenge. One of the most promising approaches is *in meso* MP crystallization, based on lipid containing crystallization matrixes, which made a key contribution to the crystallization of important proteins.[3−5] New tools of *in meso* crystallization have allowed nanovolume high throughput crystallization.[6] This together with the advances in serial crystallography at X-ray synchrotron sources and free electron lasers made crystallography with micrometer size crystals possible, but simultaneously resulted in a new challenge—imaging of extremely small crystals, especially those grown *in meso* because the crystallization matrix is visually often quite birefringent, opaque and turbid. SONICC (second order nonlinear imaging of chiral crystals) was developed as an imaging technology for identifying chiral crystals and relies on SHG (Second Harmonic Generation) and UV-TPEF (ultraviolet two photon excited fluorescence) techniques.[7−9] SONICC makes it easy to visualize microcrystals, including also optically obscured crystals buried in *in meso* matrix.[10] Nevertheless, the technique fails when there are salt crystals in the probe and/or protein crystals with high symmetry classes. In the latter case the crystals will generate poorly detectable SHG signal scattering. SHG has great advantages, however, also limitations described in the literature. In addition, at the moment there is no sufficiently cheap option of an SHG device for crystal imaging, therefore a search for new complementary approaches to crystals' studies and imaging might be very important. Iit would be especially important to develop a complementary approach allowing characterization of a specific content of the crystals (availability of cofactors, ligands, RNA and DNA and their states). In principle, all this might be done using fingerprint bands in their Raman spectra. Unfortunately, the Raman intensity is too week to work with very small crystals. We show that CARS is one of the possible complementary powerful approaches to the imaging and studying of the crystals.

We describe here a new approach, based on polarized coherent anti-Stokes Raman scattering (P-CARS) imaging of *in meso* grown MP (and also water-soluble protein) crystals. CARS microscopy provides an advanced nondestructive and label-free technique with high sensitivity and high lateral spatial resolution capable of selective chemical imaging of major types of macromolecules: proteins, lipids, nucleic acids, etc.[11,12] Like spontaneous Raman, CARS probes vibrational modes in molecules and does not require exogenous dyes or markers, which is advantageous in imaging small molecules for which labeling may strongly affect their properties.

CARS is a third-order nonlinear optical process involving interactions between a pump beam of frequency ω_p, a Stokes beam of frequency ω_s, and a CARS signal at the anti-Stokes frequency of $\omega_{as} = 2\omega_p - \omega_s$ generated in the phase matching direction. The vibrational contrast in CARS is created when the frequency difference $\Delta\omega = \omega_p - \omega_s$ between the pump and the Stokes beams is tuned to be resonant with a given vibration mode of a selected chemical bond (Figure S1). In this case, the resonant oscillators are coherently driven by the excitation fields, thereby generating a strong and directed anti-Stokes signal compared to a weak spontaneous Raman signal (most

Received: May 12, 2016
Published: September 16, 2016

DOI: 10.1021/jacs.6b04464
J. Am. Chem. Soc. 2016, 138, 13457−13460

molecules have a small Raman cross section, typically ~10^{-30} to 10^{-25} cm^2). CARS signals are 3−4 orders of magnitude stronger than those of a spontaneous Raman process.

Another advantage of CARS microscopy is an enhanced spatial resolution that is achieved with two collinearly overlapping near-infrared picosecond beams and a water-immersion objective with a high numerical aperture. Furthermore, the CARS signal is generated only from the focal volume of the objective, thus providing a natural way to perform three-dimensional sectioning without the need of confocal geometry.

It was already discussed in literature that CARS is sensitive for *in vivo* detection of lipid (cholesterol) crystals naturally occurring in the cells.[13] However, until now CARS imaging of protein crystals has not been addressed. CARS may have important advantages and complementarity to the existing protein crystals imaging techniques (for instance, SHG imaging) because it does not only image crystals but also may study the molecular composition of membrane protein crystals via the use of Raman scattering spectra lines specific for different molecules comprising a crystallization matrix and often the crystals. To have a reference for understanding the efficiency of P-CARS images, we performed complementary SHG imaging of crystals studied via CARS. The CARS and SHG images are composed of 500 × 500 pixels taken by raster scanning the sample. Signal integration time was 3 μs/pixel.

As the first step to understand the CARS imaging potential, we performed studies with *in meso* grown bacteriorhodopsin (bR) crystals. We used bR in the present work because it is the most studied membrane protein. We investigated its structure and crystallization (including the studies of merohedral twinning) in great details and developed protocols of bR crystallization allowing us to regulate the size of the crystals, their quality and level of twinning. Our data obtained with lysozyme crystals support the idea of CARS general application to imaging of the crystals of biological macromolecules. bR is a seven α-helical membrane protein of *Halobacterium salinarum*. bR is one of the most extensively studied membrane proteins during the past 40 years.[14] The protein is often used to develop new methodologies.[15−19] In all experiments, we used *in meso* grown BR crystals of $P6_3$ symmetry. The hexagonal crystal plates were with the sizes 1−100 μm in two dimensions and from about 0.5 to 20 μm thick. Very small crystals were used to estimate the limits of CARS sensitivity and spatial resolution. Bacteriorhodopsin contains a chromophore retinal. The wavelength 568 nm corresponds to the maximum of bR absorption, which is determined by the chromophore and the crystals have a characteristic purple color. The chromophore has a well studied Raman spectrum (Figure S3).[20] bR crystals were imaged directly in a crystallization well with selected C═C retinal chromophore Raman bands at 1529 and 1570 cm^{-1}.

First we compared P-CARS (polarized CARS) and F-CARS (forward CARS) images of bR crystals in the same crystallization probe. The hexagonal plane of some of the crystals is oriented along the image and some of them are perpendicular. With P-CARS (Figure S4c,d and Figure S5) the Raman bands display a higher signal to background ratio (of 30:1) in comparison with the F-CARS (about a half intensity contrast). Tuning the difference frequency $\omega_P - \omega_S$ between the pump and the Stokes beams to 1570 cm^{-1} resulted in an effective suppression of the nonresonant background in the P-CARS mode: the background signal almost disappears and even very small crystals of the in-plane size about 2 μm and the thickness less than 1 μm are well resolved. Their in-plane shape, including the edges of the crystals, is imaged with a high resolution (about 500 nm). To compare the sensitivity and resolution of P-CARS with those of the known methods (standard optical microscopy and SHG), we demonstrate in Figure 1a−f the images of the crystals of different sizes. Though

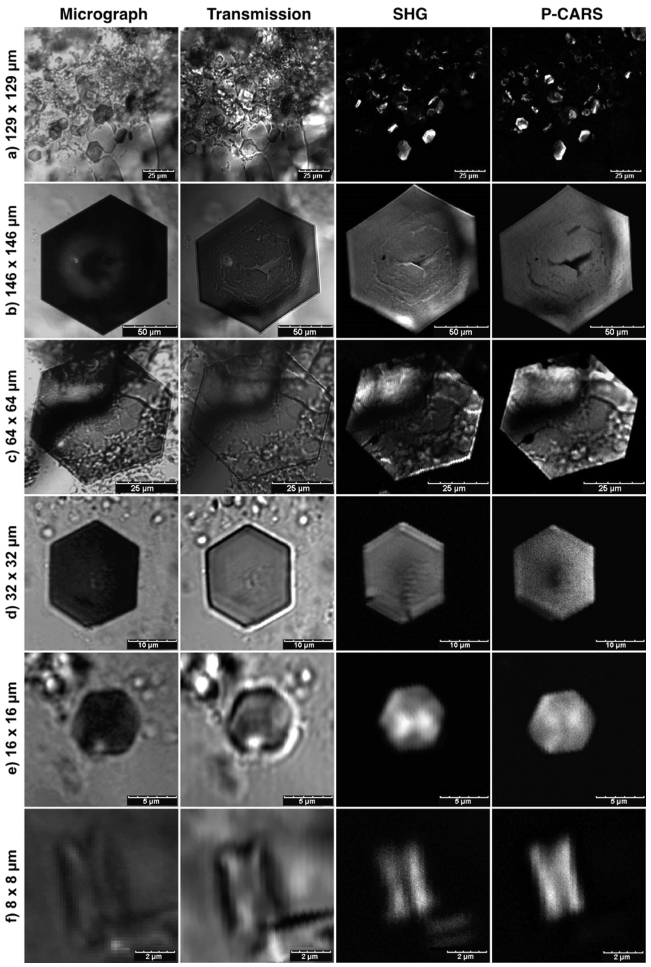

Figure 1. Gallery of micrograph, transmission, SHG and CARS images of bR crystals acquired in various modes: (a) panoramic picture of a crystallization probe, (b, c) big crystals, (d) intermediate size crystals, (e and f) very small crystals.

the difference between micrographs and transmission images is not very pronounced it is seen that the images under the monochromatic light (transmission) provide more structured images. Showing two types (micrograph and transmission) of images, we aim to demonstrate that neither of them can compete with CARS for the quality of crystal imaging. In the case of the larger ones (30 μm and greater), all the techniques visualize the crystals well. However, only CARS and SHG are able to detect the defects of the crystals and CARS does this with a better contrast (Figure 1b). In the case of smaller crystals (less than 20 μm), the advantages of CARS and SHG are even more crucial (Figure 1a). Only they are able to identify important crystal features. SHG has a strong signal when the crystals are well ordered. However, when the order is not sufficient only CARS can identify the small crystals (Figure S5). Thus, complementary application of CARS and SHG techniques provides a unique opportunity to study the growth of protein crystals on a large range of scales.

DOI: 10.1021/jacs.6b04464
J. Am. Chem. Soc. 2016, 138, 13457−13460

We observed with some of the crystals (Figures 1 and 2) that the shape and/or size of the same crystals imaged by CARS and

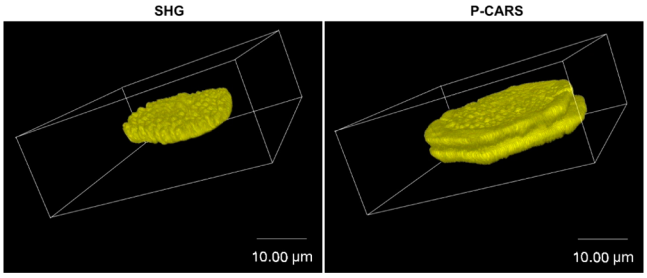

Figure 2. 3D SHG and 3D P-CARS images of a twinned bR crystal. Box size: 48 × 48 × 24 μm. Images were acquired with 6 ps laser source.

SHG are different. We suggest that it happens in cases when some parts of the crystals are not well ordered. It is known that SHG signal is strong only when the crystal is well ordered. It is of interest because a complementary use of both methods can provide information about the level of order in crystal packing and help to select crystals preliminarily for X-ray crystallography. It can be very useful because quite often the crystals may have a perfect shape but do not diffract at all.

Amazing sensitivity of the P-CARS imaging is further demonstrated by detection and imaging of merohedrally twinned bR crystals (Figure 2). Merohedral twinning is one of the most common crystal-growth defects. Neither there is a fast approach to detection of twinned crystals nor is there an efficient method of the twinning-ratio determination. Twinned crystals cannot be optically distinguished. The only reliable method to detect twinning of the crystals is X-ray crystallography,[16,17] which requires time-consuming X-ray data collection. In the present work, we studied the potential of CARS for the detection of such crystals. Figure 2 demonstrates that twinning of bR can be easily detected even in the case of small crystals with a micrometer size thickness, whereas SHG signal with 6 ps excitation hardly discriminates the morphology of the twinned crystal if it partly consists of low-ordered segments, as it is observed in our work. In contrast to X-ray crystallography, CARS makes the characterization of their morphology possible and demonstrates that the crystal consists of two nearly equal domains with the thickness about 2.5 μm. It is in line with our previous observations of two or maximum three symmetrically related nontwinned crystals.[16,17]

Finally, we applied P-CARS for imaging of lysozyme crystals. Lysozyme is a water-soluble protein also widely used in a number of investigations including the studies of mechanisms of water-soluble protein crystal growth.[21] We used a common for all the proteins Raman Amide I band at 1655 cm^{-1} to image the crystals (Figure S7) and therefore such imaging can be applied for all protein crystals. The crystals were obtained by *in meso* crystallization in the same way as bR crystals. Therefore, the crystal imaging was under the same unfavorable conditions for their observation with standard optical microscopy. Moreover, the Raman spectra were obtained (Figure S8). Despite these facts, even small crystals with the size less than 5 μm in the largest direction and about 1 μm thick were well imaged (Figure S9).

The images of lysozyme crystals with Amide I Raman band demonstrate that also in the case of this protein one can obtain high-resolution CARS images and the sensitivity is sufficiently high to detect and image very small (about 1 μm) crystals (Figure S9) as well as to see the cracks in a lysozyme crystal (not shown). In opposite, SHG images of the same crystals were unsuccessful (Figure S9). It is no surprise because these are the crystals of high symmetry $P4_32_12$ space group. In addition, we show also the images of one of the crystals done with Amide I (1655 cm^{-1}), Amide II (1555 cm^{-1}), Amide III (1340 cm^{-1}) and C−H (1445 cm^{-1}) Raman bands of the protein (Figure S10). Figures S8 and S9 illustrate a remarkable advantage of CARS to detect, image and study crystals with Raman bands specific to different molecular groups or/and molecules.

Thus, CARS, especially P-CARS, can be generally applied for fast, high resolution, high contrast and very informative imaging of protein crystals. The CARS and SHG images are composed of 500 × 500 pixels taken by raster scanning the sample. Signal integration time was 3 μs/pixel.

■ ASSOCIATED CONTENT

Supporting Information

The Supporting Information is available free of charge on the ACS Publications website at DOI: 10.1021/jacs.6b04464.

Details of experiments (PDF)

■ AUTHOR INFORMATION

Corresponding Authors

*G.M.A. arzuman@jinr.ru
*V.I.G. valentin.gordeliy@ibs.fr

Notes

The authors declare no competing financial interest.

■ ACKNOWLEDGMENTS

The work was supported by the CEA(IBS) − HGF(FZJ) STC 5.1 specific agreement. The work was supported by RSF 16-15-00242. This work used the platforms of the Grenoble Instruct Center (ISBG: UMS 3518 CNRS-CEA-UJF-EMBL) with support from FRISBI (ANR-10-INSB-05-02) and GRAL (ANR-10-LABX-49-01) within the Grenoble Partnership for Structural Biology (PSB). A. Round is greatly acknowledged for careful reading of the paper and his very valuable comments.

■ REFERENCES

(1) Krogh, A.; Larsson, B.; von Heijne, G.; Sonnhammer, E. L. J. *J. Mol. Biol.* **2001**, *305*, 567−580.
(2) Overington, J. P.; Al-Lazikani, B.; Hopkins, A. L. *Nat. Rev. Drug Discovery* **2006**, *5*, 993−6.
(3) Pebay-Peyroula, E.; Rummel, G.; Rosenbusch, J. P.; Landau, E. M. *Science (Washington, DC, U. S.)* **1997**, *277*, 1676−1681.
(4) Gordeliy, V. I.; Labahn, J.; Moukhametzianov, R.; Efremov, R.; Granzin, J.; Schlesinger, R.; Büldt, G.; Savopol, T. J.; Scheidig, A. P.; Klare, J.; Engelhard, M. *Nature* **2002**, *419*, 484−7.
(5) Rosenbaum, D. M.; Cherezov, V.; Hanson, M. A.; Rasmussen, S. G.; Thian, F. S.; Kobilka, T. S.; Choi, H. G.; Yao, X. J.; Weis, W. I.; Stevens, R. C.; Kobilka, B. K. *Science* **2007**, *318*, 1266−73.
(6) Caffrey, M.; Cherezov, V. *Nat. Protoc.* **2009**, *4*, 706−31.
(7) Wampler, R. D.; Kissick, D. J.; Dehen, C. J.; Gualtieri, E. J.; Wang, H.-F.; Thompson, D. H.; Cheng, J.-X.; Simpson, G. J.; Grey, J. *J. Am. Chem. Soc.* **2008**, *130* (43), 14076−14077.
(8) Closser, R. G.; Gualtieri, E. J.; Newman, J. A.; Simpson, G. J. *J. Appl. Crystallogr.* **2013**, *46*, 1903−1906.
(9) Haupert, L. M.; DeWalt, E. L.; Simpson, G. J. *Acta Crystallogr., Sect. D: Biol. Crystallogr.* **2012**, *68* (11), 1513−1521.

DOI: 10.1021/jacs.6b04464
J. Am. Chem. Soc. 2016, 138, 13457−13460

(10) Bogorodskiy, A.; Frolov, F.; Mishin, A.; Round, E.; Polovinkin, V.; Cherezov, V.; Gordeliy, V.; Büldt, G.; Gensch, T.; Borshchevskiy, V. *Cryst. Growth Des.* **2015**, *15* (12), 5656−5660.
(11) Zumbusch, A.; Holtom, G.; Xie, X. *Phys. Rev. Lett.* **1999**, *82*, 4142−4145.
(12) Krafft, C.; Ramoji, A. A.; Bielecki, C.; Vogler, N.; Meyer, T.; Akimov, D.; Rösch, P.; Schmitt, M.; Dietzek, B.; Petersen, I.; Stallmach, A.; Popp, J. *J. Biophotonics* **2009**, *2*, 303−312.
(13) Suhalim, J. L.; Chung, C. Y.; Lilledahl, M. B.; Lim, R. S.; Levi, M.; Tromberg, B. J.; Potma, E. O. *Biophys. J.* **2012**, *102*, 1988−1995.
(14) Lanyi, J. K. *Biochim. Biophys. Acta, Bioenerg.* **2004**, *1658*, 14−22.
(15) Landau, E. M.; Rosenbusch, J. P. *Proc. Natl. Acad. Sci. U. S. A.* **1996**, *93*, 14532−5.
(16) Borshchevskiy, V.; Efremov, R.; Moiseeva, E.; Büldt, G.; Gordeliy, V. *Acta Crystallogr., Sect. D: Biol. Crystallogr.* **2010**, *66*, 26−32.
(17) Efremov, R.; Moukhametzianov, R.; Büldt, G.; Gordeliy, V. *Biophys. J.* **2004**, *87*, 3608−13.
(18) Borshchevskiy, V.; Round, E.; Erofeev, I.; Weik, M.; Ishchenko, A.; Gushchin, I.; Mishin, A.; Willbold, D.; Büldt, G.; Gordeliy, V. *Acta Crystallogr., Sect. D: Biol. Crystallogr.* **2014**, *70*, 2675−2685.
(19) Borshchevskiy, V. I.; Round, E. S.; Popov, A. N.; Büldt, G.; Gordeliy, V. I. *J. Mol. Biol.* **2011**, *409*, 813−25.
(20) Lewis, A.; Spoonhower, J.; Bogomolni, R. A.; Lozier, R. H.; Stoeckenius, W. *Proc. Natl. Acad. Sci. U. S. A.* **1974**, *71*, 4462−4466.
(21) Gushchin, I.; Chervakov, P.; Kuzmichev, P.; Popov, A. N.; Round, E.; Borshchevskiy, V.; Ishchenko, A.; Petrovskaya, L.; Chupin, V.; Dolgikh, D. A.; Arseniev, A. S.; Kirpichnikov, M.; Gordeliy, V. *Proc. Natl. Acad. Sci. U. S. A.* **2013**, *110*, 12631−12636.

DOI: 10.1021/jacs.6b04464
J. Am. Chem. Soc. 2016, 138, 13457−13460